

On the Design of Phase Locked Loop Oscillatory Neural Networks: Mitigation of Transmission Delay Effects

Rongye Shi, Thomas C. Jackson, Brian Swenson, Soummya Kar, Lawrence Pileggi

Department of Electrical and Computer Engineering

Carnegie Mellon University

Pittsburgh, PA 15213 USA

{rongyes, thomasj, brianswe, soummyak, pileggi}@andrew.cmu.edu

Abstract—This paper introduces a novel design of phase locked loop (PLL) based oscillatory neural networks (ONNs) to mitigate the frequency clustering phenomenon caused by transmission delays in real systems. Theoretical analysis of the ONN reveals that transmission delays can produce frequency clustering that leads to synchronization and convergence failure. This paper describes the redesign of ONN dynamics and associated system-level architecture to achieve robustness. Specifically, we first demonstrate that using the phase information of zero-crossing points of inputs as the PLL error signal enables the ONN dynamical model to correctly synchronize under uniform transmission delays. A Type-II PLL based ONN architecture is shown via simulation to provide this property in hardware. Furthermore, to accommodate non-uniform transmission delays in hardware, a phase synchronization technique is proposed that is shown to provide the correct synchronization behavior.

Keywords—associative memory, oscillatory neural network, pattern recognition, phase locked loops, transmission delay

I. INTRODUCTION

Various architectures and hardware implementations of neural networks (NNs) have been proposed and studied [1, 2, 3]. Many NN architectures are based on voltage or current amplitudes [4, 5] as the state variables, however, the oscillatory neural network (ONN) is a promising architecture, inspired by the observation of synchronous oscillatory behavior of the brain, that uses phase as the state variable and scales the phase contribution by scaling the amplitudes of the contributing signals. This feature of ONN hardware design makes it less sensitive to gain error and voltage/current offset, which can simplify the corresponding circuit hardware complexity and lower power requirements.

The ONN architecture considered in this paper is comprised of coupled phase locked loops (PLLs), as proposed in [6]. PLLs are the signal processing units (neurons), and the ONN can serve as an associative memory where all PLLs synchronize and their phase relations correspond to a memorized pattern in the system. Efficient implementations of oscillators have been explored based on emerging technologies [7,8] to facilitate the scaling of such NNs to large problem sizes. However, we will show that some unexpected phenomena occur when implementing these systems in hardware. Specifically, the transmission

delays among the “synapses” have a significant impact on the convergence properties of the system proposed in [6].

In this paper, we study the impact of transmission delays on ONN systems, and then propose solutions to overcome these limitations for actual hardware system implementations. The main contributions of the paper are as follows:

- 1) *Identify and describe the frequency clustering phenomenon:* Analytical evidence, which is supported with the system-level simulations, reveals that transmission delays cause the ONN neurons to divide into multiple frequency clusters instead of synchronizing to a single frequency. Even systems with uniform transmission delays display this behavior. We term this frequency clustering.
- 2) *ONN model based on zero-crossing phase detectors:* We mathematically show that using the phase information of zero-crossing points of inputs as the source of error signal for the PLL, the ONN dynamical model can correctly synchronize under uniform transmission delays.
- 3) *Design of the Type-II PLL ONN architecture:* We propose a practical implementation to achieve the aforementioned model in hardware. The proposed Type-II PLL ONN is shown to be robust against uniform transmission delays.
- 4) *Hardware to accommodate random transmission delays:* A phase correction technique is proposed to “snap” the random delays to a quantized value, such that the effective transmission delays to each neuron are uniform. This makes the Type-II PLL ONN much more robust with respect to random transmission delays for actual systems.

II. OSCILLATORY NEURAL NETWORK IMPLEMENTATION CHALLENGES

A. Original ONN Architecture

The structure of the original ONN architecture proposed in [6] is shown in Fig. 1. Each of the n neurons is composed of a PLL with a multiplier as the phase detector and a 90 degree phase shifter at the output. The network is fully connected which means that each neuron is coupled to every other neuron via a synapse. In the i^{th} PLL, the output signal I_i from the multiplier (phase detector) is

This work was supported in part by Systems on Nanoscale Information fabriCs (SONIC), one of the six SRC STARnet Centers.

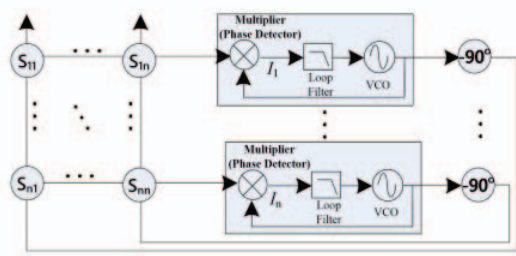


Fig. 1 Original structure of the oscillatory neural network using multiplier PLL's as neurons.

$$I_i = \sum_{j=1}^n s_{ij} V(\theta_j) V(\theta_j - \pi/2), \quad (1)$$

where θ_i is the total phase of the voltage controlled oscillator (VCO) in the i^{th} PLL, and s_{ij} are the synaptic weights [6]. V is a 2π -periodic waveform satisfying the “odd-even” condition: $V(\theta)$ is an odd function, whereas $V(\theta - \pi/2)$ is an even function. The phase state θ_i can be represented as $\theta_i(t) = \Omega t + \varphi_i$, where $\Omega \gg 1$ is the natural frequency and φ_i is the phase deviation of the i^{th} PLL from the natural phase Ωt . Using averaging and Fourier analysis, we can describe the dynamics of the ONN depicted in Fig. 1 as

$$\dot{\varphi}_i = \sum_{j=1}^n s_{ij} H(\varphi_j - \varphi_i). \quad (2)$$

$H(\varphi_j - \varphi_i)$ is the averaged result of the loop filter and is given by:

$$H(\varphi_j - \varphi_i) = \lim_{T \rightarrow \infty} \frac{1}{T} \int_0^T V(\Omega t + \varphi_i) V(\Omega t + \varphi_j - \pi/2) dt \\ = \sum_{m=1,3,5,\dots}^{\infty} \frac{a_m^2}{2} (-1)^{(m-1)/2} \sin m(\varphi_j - \varphi_i), \quad (3)$$

where a_m is Fourier coefficient of the m^{th} harmonic of $V(\theta)$. If the synapse matrix is symmetric, i.e., $s_{ij} = s_{ji}$, then the system will converge and synchronize to the same frequency with stable phase relationships that are dependent on the synaptic weight. More details of this analysis are in [6].

This property enables the ONN to memorize and retrieve different patterns. The patterns can be trained into the network by producing the values of synaptic weights s_{ij} through a learning algorithm. One simple algorithm is the Hebbian training rule which is given by

$$s_{ij} = \frac{1}{n} \sum_{k=1}^P \xi_i^k \xi_j^k, \quad (4)$$

where $\xi^k = (\xi_1^k, \xi_2^k, \dots, \xi_n^k)$ is the n dimensional vector representing the k^{th} pattern stored in the network. The storage of binary patterns is considered, so $\xi_i^k = \pm 1$. For these systems, one neuron is chosen as the reference. If φ_i is the reference phase, ξ_i^k is fixed to be 1, then $\xi_j^k = 1$ corresponds to $\varphi_i = \varphi_j$ (in-phase case) and $\xi_j^k = -1$ corresponds to $\varphi_i = \varphi_j + \pi$ (anti-phase case). Using this training rule, the symmetry of synapse matrix is guaranteed. The algorithm attempts to set the patterns as stable equilibrium points of (2). If this is the case, when the system is initialized with a distorted pattern near the memorized pattern, the system will

typically converge to the correct stored phase relations.

A multiplier-based ONN with 20 neurons was built in Simulink to test the architecture. The VCOs are set to operate at the natural frequency of 1 GHz. The network was trained to memorize the two patterns shown in Fig. 2. The simulation shows that with a distorted input, for 1GHz VCOs, the ONN recognition time is about 400 times the VCO period (400 ns).

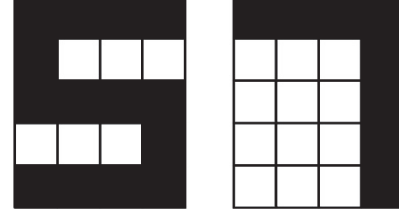


Fig. 2 Two patterns are stored in the 20-neuron ONN. If neuron one serves as the reference, then black pixels represent neurons with 0 degree phase relation w.r.t neuron one, while white pixels represent neurons with 180 degree phase relation w.r.t neuron one.

For the retrieval of a correct pattern, two things must be true:

- 1) The ONN globally synchronizes at one frequency. Fig. 3(a) tracks the VCO control voltage of all 20 neurons. The VCO control voltage is proportional to the output frequency. At the end of the evolution stage, every neuron shares the same VCO control voltage, which means that every oscillator generates the same frequency.
- 2) The phase relationships converge to the correct pattern. As shown in Fig. 3(b), entering the evolution stage, the system starts from a distorted image “5” and, at the end of the evolution stage, the output converges to the memorized correct pattern.

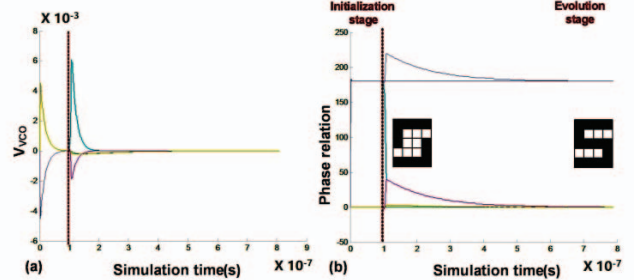


Fig. 3 (a) VCO control voltage (V_{VCO}) vs. simulation time. Since V_{VCO} is proportional to the output frequency deviation from Ω , the curves precisely reflect the frequency deviation vs. time. (b) Phase relation vs. simulation time.

Despite significant theoretical study of these systems in [9] and [10], and proposed systems using emerging technologies [7], there have been no known fabricated IC implementations. When considering hardware design, we must include details that limit physical implementation, and redesign the system as necessary under these constraints. Specifically, this work considers unavoidable transmission delays in a physical network.

B. The Cause of the Frequency Clustering Phenomenon

When considering transmission delays, we observe an

unexpected desynchronization phenomenon. The model of ONN with delays is shown in Fig. 4. In this model, delays are placed before each neuron and the delay vector $\delta\hat{\varphi}$ can be used to represent the accumulated effect of transmission delay over the entire network. The study of this model can be generalized to any ONN with delays.

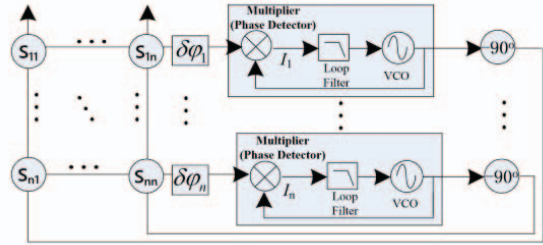


Fig. 4 ONN with transmission delays ($\delta\varphi_1, \dots, \delta\varphi_n$).

We consider the model in Fig. 4, where phase detectors are multipliers. Taking transmission delays $\delta\hat{\varphi} = (\delta\varphi_1, \dots, \delta\varphi_n)$ into account, the differential equation (2) needs to be revised. Because the summed signal for the i^{th} neuron is shifted by $\delta\varphi_i$, φ_j should be replaced by $(\varphi_j - \delta\varphi_i)$. Then the dynamics of the ONN with transmission delays is described as

$$\dot{\varphi}_i = \sum_{j=1}^n s_{ij} H(\varphi_j - \varphi_i + \delta\varphi_i). \quad (5)$$

Generally, the memorized patterns may no longer be stable due to the transmission delays and there may not be an equilibrium near the memorized pattern. This is the reason why the system cannot synchronize, let alone converge to the memorized pattern. For this claim, let the system initialize from one of the memorized patterns:

$$\dot{\varphi}_i = \sum_{j=1}^n s_{ij} H(\varphi_j^* - \varphi_i^* + \delta\varphi_i) = \sum_{j=1}^n c_{ij} H(\delta\varphi_i), \quad (6)$$

$$c_{ij} = s_{ij} e^{i(\varphi_j^* - \varphi_i^*)}. \quad (7)$$

Since (6) is nonzero with different values for different neurons, the frequencies do not synchronize at the pattern.

System-level simulation confirms that these transmission delays may cause the neurons to settle to different frequencies from one another, meaning neither condition for correct recovery is met.

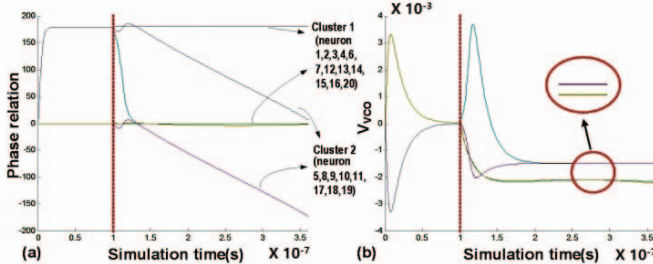


Fig. 5 Performance of ONN with uniform transmission delays.

Fig. 5 shows a simple example, where the ONN has uniform transmission delays. Fig. 5(a) tracks the phase relation with respect to neuron 1 and it can be seen that the curves split into 2 clusters. Fig. 5(b) tracks VCO control voltage. We can observe 2 different control voltage levels,

which indicate that the system settles to 2 different frequencies. We refer to this as a *frequency clustering* phenomenon.

We change the delay vector $\delta\hat{\varphi}$ ($\delta\varphi_1, \dots, \delta\varphi_n$) and record the performance with the same synaptic network to see if there is any relation between $\delta\hat{\varphi}$ and clustering. Some empirically discovered properties are summarized here:

- 1) No matter how $\delta\hat{\varphi}$ is changed (small delays below 30 degrees are considered in this paper), once the clusters occur, the system can always be divided into two clusters with exactly the same distribution, as in Fig. 5(a). Moreover, the number of clusters is a function of the weight pattern.
- 2) In each cluster, the correct pattern is preserved with the delta phase caused by the delay. Specifically, neurons in one cluster approximately have the following phase relation: $(\varphi_i - \varphi_j) = (\varphi_i^* - \varphi_j^* + \delta\varphi_i - \delta\varphi_j)$, where $\varphi_j^* = 0$ for $\xi_j = 1$ and $\varphi_j^* = 180^\circ$ for $\xi_j = -1$. Here, $(\varphi_1^*, \dots, \varphi_n^*)$ is the pattern the system will converge to from its initial condition in absence of transmission delays and we call it the *objective pattern*.

Note that even with uniform delays, the ONN does not synchronize properly. Transmission delays are unavoidable in a real system. For instance, a physical ONN has an effective low pass filter (LPF) at the input of each PLL neuron due to parasitic capacitance. Various non-ideal effects derived from parasitics exist in any hardware implementation and cause some transmission delays (phase shifts) in signal. The inevitability of the transmission delays which cause the clustering phenomenon threatens the elegance of using this ONN to perform pattern recognition.

C. Theoretical Evidence for Frequency Clustering

We provide theoretical evidence for clustering to improve our understanding of this phenomenon. Instead of complete desynchronization, in simulation the oscillators form “clusters”. Similar to what has been described in [11], the neurons are divided into groups. Within each group, neurons are synchronous, but there is no synchrony between groups.

A clustered solution has been observed and summarized in the simulation: neurons within the same cluster have the phase relation of $(\varphi_i - \varphi_j) = (\varphi_i^* - \varphi_j^* + \delta\varphi_i - \delta\varphi_j)$. Since $\delta\varphi_j$ is relatively small, this phase point is close to the memorized pattern point. We center the representative point of this phase relation:

$$(\varphi_1^* + \delta\varphi_1, \dots, \varphi_n^* + \delta\varphi_n). \quad (8)$$

Note (8) may not be stable, and we call it the *quasi-equilibrium point*. We define

$$\varphi_i'' = \varphi_i' + \varphi_i^* = \varphi_i'' + \varphi_i^* + \delta\varphi_i. \quad (9)$$

Then, (5) becomes

$$\begin{aligned} \dot{\varphi}_i'' &= \sum_{j=1}^n s_{ij} H(\varphi_j'' - \varphi_i'' + \varphi_j^* - \varphi_i^* + \delta\varphi_j - \delta\varphi_i + \delta\varphi_i) \\ &= \sum_{j=1}^n s_{ij} H(\varphi_j'' - \varphi_i'' + \varphi_j^* - \varphi_i^* + \delta\varphi_j). \end{aligned} \quad (10)$$

The term $\delta\varphi_j$ remaining in (10) is the transmission delay attached to the j^{th} neuron, not the i^{th} neuron itself. It has been fully illustrated in [6] that H (see (3)) is a 2π -periodic odd

function, so that (10) can be further simplified by pulling the pattern term $(\varphi_i^* - \varphi_j^*)$ out of H :

$$\dot{\varphi}_i'' = \sum_{j=1}^n c_{ij} H(\varphi_j'' - \varphi_i'' + \delta\varphi_j), \quad c_{ij} = s_{ij} e^{i(\varphi_i^* - \varphi_j^*)}. \quad (11)$$

At the point of (8), $(\varphi_j'' - \varphi_i'') = 0$, and (11) becomes

$$\dot{\varphi}_i'' = \sum_{j=1}^n c_{ij} H(\delta\varphi_j). \quad (12)$$

We denote this value as ω_i^* which represents the frequency deviation from natural frequency Ω at (8). The matrix made up of c_{ij} is denoted as \mathbf{C} .

We observe that the cluster distribution matches properties of the matrix \mathbf{C} : as long as the i^{th} row is the same to the j^{th} row in the matrix \mathbf{C} , neuron i and neuron j evolve to the same cluster in the simulation. For example, if the network is trained with the patterns “5” and “7” shown in Fig. 2, the synapse matrix is determined by the Hebbian rule (the term $1/n$ does not affect the conclusion and is temporarily ignored here). When image “5” is the objective pattern, according to (7) and (11), matrix \mathbf{C} can be determined by scaling the synapse matrix with pattern “5”. We give the complete matrix \mathbf{C} for this specific case in Fig. 6 for visualization.

2	2	2	2	2	0	2	2	0	0	0	2	2	2	2	2	2	0	0	0	2
2	2	2	2	0	2	2	0	0	0	0	2	2	2	2	2	2	0	0	0	2
2	2	2	2	0	2	2	0	0	0	0	2	2	2	2	2	2	0	0	0	2
2	2	2	2	0	2	2	0	0	0	0	2	2	2	2	2	2	0	0	0	2
2	2	2	2	0	2	2	0	0	0	0	2	2	2	2	2	2	0	0	0	2
0	0	0	0	2	0	2	2	2	0	0	0	2	2	2	2	2	0	0	2	2
2	2	2	2	0	2	2	0	0	0	0	2	2	2	2	2	2	0	0	0	2
2	2	2	2	0	2	2	0	0	0	0	2	2	2	2	2	2	0	0	0	2
2	2	2	2	0	2	2	0	0	0	0	2	2	2	2	2	2	0	0	0	2
2	2	2	2	0	2	2	0	0	0	0	2	2	2	2	2	2	0	0	0	2
0	0	0	0	2	0	2	2	2	0	0	0	0	2	2	2	2	0	0	2	2
0	0	0	0	2	0	2	2	2	0	0	0	0	2	2	2	2	0	0	2	2
0	0	0	0	2	0	2	2	2	0	0	0	0	2	2	2	2	0	0	2	2
2	2	2	2	0	2	2	0	0	0	0	2	2	2	2	2	2	0	0	0	2
2	2	2	2	0	2	2	0	0	0	0	2	2	2	2	2	2	0	0	0	2
2	2	2	2	0	2	2	0	0	0	0	2	2	2	2	2	2	0	0	0	2
2	2	2	2	0	2	2	0	0	0	0	2	2	2	2	2	2	0	0	0	2
2	2	2	2	0	2	2	0	0	0	0	2	2	2	2	2	2	0	0	0	2
0	0	0	0	2	0	2	2	2	0	0	0	0	2	2	2	2	0	0	2	2
0	0	0	0	2	0	2	2	2	0	0	0	0	2	2	2	2	0	0	2	2
0	0	0	0	2	0	2	2	2	0	0	0	0	2	2	2	2	0	0	2	2
2	2	2	2	0	2	2	0	0	0	0	2	2	2	2	2	2	0	0	0	2

Fig. 6 Content of matrix \mathbf{C} determined by pattern “5” and “7” with “5” as the objective pattern. Red boxes indicate that row 5, 8, 9, 10, 11, 17, 18 and 19 are identical which implies that corresponding neurons will evolve into the same cluster.

We can see that in (12), if the i^{th} row and the j^{th} row are identical in \mathbf{C} , no matter how $\delta\hat{\varphi}$ is changed, we can always get to $\omega_i^* = \omega_j^*$ at point (8). As a result, neuron i and j synchronize with the phase relation of $(\varphi_i^* - \varphi_j^* + \delta\varphi_i - \delta\varphi_j)$. Such evidence suggests that \mathbf{C} imposes intrinsic bind on neurons to form clusters.

In Fig. 6, matrix \mathbf{C} implies the following clusters: cluster 1 \mathbf{G}_1 (neuron 1, 2, 3, 4, 6, 7, 12, 13, 14, 15, 16, 20) and cluster 2 \mathbf{G}_2 (neuron 5, 8, 9, 10, 11, 17, 18, 19). In each cluster, corresponding rows are identical. In the same way, we can find out the clustering distribution with “7” as the objective pattern. The same result was repeated for different stored memories.

III. ZERO-CROSSING PHASE DETECTION ONN MODEL

Now we know that memorized patterns are no longer synchronously stable and the frequencies may cluster into multiple groups in the presence of transmission delays. This might pose difficulties for NN hardware designers, since for different memories and initial conditions, both the number of clusters and cluster distribution may vary, which makes

the performance of the ONN hard to predict. What’s worse, without synchronization, the output phase cannot be meaningfully compared. Thus, we need to explore new approaches to alleviate this problem. Here, we propose an ONN model that uses zero-crossing phase detectors and show that the proposed model is robust against uniform transmission delays.

A. Dynamical Equation of the Proposed Model

The zero-crossing phase detector (PD) detects the phase difference between the input signal and the output feedback signal by measuring the zero-crossing. The conceptual structure of the PLL neuron is as follows:

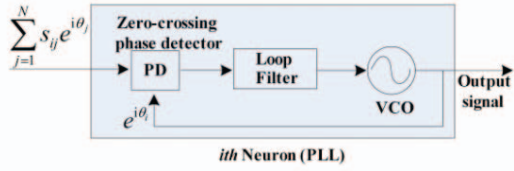


Fig. 7 The conceptual structure of the PLL equipped with zero-crossing phase detector.

Inside the neuron, the zero-crossing phase detector detects the phase difference for the *rising* zero-crossing point of the input signal and the output feedback signal. The PD generates the error signal, which is a rectangular wave with its width proportional to the phase difference. The loop filter integrates the error signal and generates control voltage for the VCO. The VCO frequency is proportional to the control voltage.

Define the zero-crossing phase of the input signal as:

$$\theta_{cross,i} = \theta_{cross}(\hat{s}_i, \hat{\theta}), \quad (13)$$

where $\hat{s}_i = (s_{i1}, s_{i2}, \dots, s_{in})$ and $\hat{\theta}$ is the phase state variable vector composed of θ_i . Then the dynamics of the i^{th} neuron is presented as

$$\dot{\theta}_i = f_i(\hat{\theta}) = k[\theta_{cross,i} - \theta_i], \quad (14)$$

where k is a positive constant. The averaging effect of the loop filter is simplified as an integral. Equation (14) constitutes a linear dynamical model w.r.t. $\theta_{cross,i}$ and the linear relation holds for $[\theta_{cross,i} - \theta_i] \in (-360^\circ, 360^\circ]$. Note $\theta_{cross,i} = \theta_{cross}(\hat{s}_i, \hat{\theta})$ is nonlinear w.r.t. $\hat{\theta}$.

In the ONN system, each neuron observes the input signals in its *egocentric* reference frame and processes the signals in a self-referential way. Since neuron i treats itself as the reference, the input zero-crossing phase observed by neuron i appears to be $\theta_{cross}(\hat{s}_i, \hat{\theta} - \theta_i \vec{1})$, and the corresponding dynamics is

$$\dot{\theta}_i = k[\theta_{cross}(\hat{s}_i, \hat{\theta} - \theta_i \vec{1})]. \quad (15)$$

For ease of analysis, we use the sine waveform as the information carrier. With the sine waveform, the input summed signal is

$$\sum_{j=1}^N s_{ij} e^{i\theta_j} = \sum_{j=1}^N s_{ij} \cos \theta_j + i \sum_{j=1}^N s_{ij} \sin \theta_j. \quad (16)$$

From the viewpoint of neuron i , the input signal appears to be

$$\sum_{j=1}^N s_{ij} e^{i(\theta_j - \theta_i)} = \sum_{j=1}^N s_{ij} \cos(\theta_j - \theta_i) + i \sum_{j=1}^N s_{ij} \sin(\theta_j - \theta_i). \quad (17)$$

Under the Hebbian learning rule, if a binary pattern $\hat{\theta}^*$ (contains only 0 or 180 degree) is stored as an equilibrium, it is necessary that $\forall i, \theta_{cross} \left(\sum_{j=1}^N s_{ij} e^{i(\theta_j^* - \theta_i^*)} \right) = 0$. At the memorized pattern $\hat{\theta}^*$, there is no difference between the zero-crossing phase and the phase of the i^{th} neuron itself, and thus no error signal will be generated. As an effective approximation, the phase of the zero-crossing point of the input summed signal can be calculated using the *atan2* function. The definition of *atan2* function in terms of *arctan* is

$$\text{atan2}(y, x) = \begin{cases} \arctan(y/x) & \text{if } x > 0 \\ \arctan(y/x) + \pi & \text{if } x < 0 \text{ and } y \geq 0 \\ \arctan(y/x) - \pi & \text{if } x < 0 \text{ and } y < 0 \\ +\pi/2 & \text{if } x = 0 \text{ and } y > 0 \\ -\pi/2 & \text{if } x = 0 \text{ and } y < 0 \\ \text{undefined} & \text{if } x = 0 \text{ and } y = 0 \end{cases}.$$

In the complex plane, the input signal (16) is represented as $(\sum_{j=1}^N s_{ij} \cos(\theta_j - \theta_i), \sum_{j=1}^N s_{ij} \sin(\theta_j - \theta_i))$, and the phase of the zero-crossing point in terms of *atan2* is

$$\theta_{cross}(\hat{s}_i, \hat{\theta} - \theta_i \vec{1}) = \text{atan2}\left(\sum_{j=1}^N s_{ij} \sin(\theta_j - \theta_i), \sum_{j=1}^N s_{ij} \cos(\theta_j - \theta_i)\right). \quad (18)$$

The equation (18) implies that in order to ensure $\forall i, \theta_{cross} \left(\sum_{j=1}^N s_{ij} e^{i(\theta_j^* - \theta_i^*)} \right) = 0$, based on the definition of *atan2* ($x > 0$ is required for $\text{atan2}(y, x) = 0$), $\forall i, \sum_{j=1}^N s_{ij} \cos(\theta_j^* - \theta_i^*) > 0$ is a necessary condition (not sufficient) for a binary pattern $\hat{\theta}^*$ to be successfully memorized into the network. In the rest of the paper, we define

$$\lambda_i = \sum_{j=1}^N s_{ij} \cos(\theta_j^* - \theta_i^*). \quad (19)$$

Thus, $\forall i, \lambda_i > 0$ should hold for every valid memorized pattern. When discussing the dynamics near one of the memorized patterns, we impose a small perturbation $\hat{\theta}$ to $\hat{\theta}^*$. Define $\theta_{ij} = \theta_i - \theta_j$ where θ_i is the i^{th} element of the perturbation $\hat{\theta}$. Then (18) becomes

$$\begin{aligned} \theta_{cross}(\hat{s}_i, \hat{\theta}^* + \hat{\theta} - (\theta_i^* + \theta_i) \vec{1}) \\ = \text{atan2}\left(\sum_{j=1}^N s_{ij} \sin(\theta_{ji}^* + \theta_{ji}), \sum_{j=1}^N s_{ij} \cos(\theta_{ji}^* + \theta_{ji})\right). \end{aligned} \quad (20)$$

Around the memorized pattern $\hat{\theta}^*$, $\forall i, \sum_{j=1}^N s_{ij} \cos(\theta_j^* - \theta_i^*) > 0$ holds. According to the definition of *atan2*, the dynamics of (15) is

$$\begin{aligned} \dot{\theta}_i &= f_i(\hat{\theta}^* + \hat{\theta}) = k \theta_{cross}(\hat{s}_i, (\hat{\theta}^* + \hat{\theta}) - (\theta_i^* + \theta_i) \vec{1}) \\ &= k \cdot \arctan\left[\sum_{j=1}^N s_{ij} \sin(\theta_{ji}^* + \theta_{ji}) / \sum_{j=1}^N s_{ij} \cos(\theta_{ji}^* + \theta_{ji})\right]. \end{aligned} \quad (21)$$

The first order derivative of f_i at $\hat{\theta}^*$ is

$$\begin{aligned} \frac{\partial f_i}{\partial \theta_j} \Big|_{\theta_j=0} &= \frac{\partial}{\partial \theta_j} \arctan\left(\sum_{j=1}^N s_{ij} \sin(\theta_{ji}^* + \theta_{ji}) / \sum_{j=1}^N s_{ij} \cos(\theta_{ji}^* + \theta_{ji})\right) \Big|_{\theta_j=0} \\ &= \frac{\left(\sum_{j=1}^N s_{ij} \sin \theta_{ji}^*\right)^2}{1 + \left(\sum_{j=1}^N s_{ij} \cos \theta_{ji}^*\right)^2}^{-1} \left(\frac{s_{ij} \cos \theta_{ji}^*}{\sum_{j=1}^N s_{ij} \cos \theta_{ji}^*} + \frac{\left(\sum_{j=1}^N s_{ij} \sin \theta_{ji}^*\right)^2}{\left(\sum_{j=1}^N s_{ij} \cos \theta_{ji}^*\right)^2} \right) \\ &= \frac{c_{ij}}{\sum_{j=1}^N c_{ij}} = \frac{c_{ij}}{\lambda_i}. \end{aligned} \quad (22)$$

Specifically, $\frac{\partial f_i}{\partial \theta_i} \Big|_{\theta_i=0} = \left(\frac{c_{ii}}{\lambda_i} - \sum_{j=1}^N \frac{c_{ij}}{\lambda_i} \right) = \left(\frac{c_{ii}}{\lambda_i} - 1 \right)$. Note $f_i(\hat{\theta}^*) = 0$.

We can approximate the nonlinear system (21) by its linearization about the equilibrium $\hat{\theta}^*$:

$$\dot{\theta}_i = f_i(\hat{\theta}^* + \hat{\theta}) = \left(k \sum_{j=1}^N \frac{c_{ij}}{\lambda_i} \theta_j \right) - k \theta_i = k \sum_{j=1}^N \frac{c_{ij}}{\lambda_i} (\theta_j - \theta_i). \quad (23)$$

In (23), we can see that the normalization term λ_i appears in the dynamics which indicates that the proposed ONN processes the input signal in a normalized way.

B. Stability of Memorized Patterns

As far as pattern recognition is concerned, we do not care about the absolute value of the phase of each neuron, what we care about is whether or not the phase relation can correctly converge to the memorized pattern.

Using neuron 1 as reference, we discuss the dynamics w.r.t. the phase difference between each neuron and neuron 1. Define $y_i = \theta_i - \theta_1$, and $y_{ij} = y_i - y_j$. Then $\hat{y} = \hat{\theta} - \theta_1 \vec{1}$. Additionally, $\theta_{ij} = (\theta_i - \theta_1) - (\theta_j - \theta_1) = y_i - y_j = y_{ij}$. Note that $y_1 = 0$. We get to the dynamics of the system in the form of \hat{y} :

$$\begin{aligned} \dot{y}_i &= \dot{\theta}_i - \dot{\theta}_1 = k \sum_{j=1}^N \frac{c_{ij}}{\lambda_i} (y_j - y_i) - k \sum_{j=1}^N \frac{c_{1j}}{\lambda_1} (y_j - y_1) \\ &= k \left[\left(\sum_{j=1}^N \left(\frac{c_{ij}}{\lambda_i} - \frac{c_{1j}}{\lambda_1} \right) y_j \right) - y_i + y_1 \right] \end{aligned} \quad (24)$$

Since we treat neuron 1 as reference, we have $y_1 = 0$, and the degree of freedom of (24) is $N-1$. Then

$$\dot{y}_i = k \left[\left(\sum_{j=2}^N \left(\frac{c_{ij}}{\lambda_i} - \frac{c_{1j}}{\lambda_1} \right) y_j \right) - y_i \right], \quad (i = 2, \dots, N). \quad (25)$$

The dynamics of the system near the memorized pattern is

$$\dot{\hat{y}}_{i=1} = \begin{bmatrix} \dot{y}_2 \\ \dot{y}_3 \\ \vdots \\ \dot{y}_n \end{bmatrix} = k \begin{bmatrix} \left(\frac{c_{22}}{\lambda_2} - \frac{c_{12}}{\lambda_1}\right) - 1 & \left(\frac{c_{23}}{\lambda_2} - \frac{c_{13}}{\lambda_1}\right) & \dots & \left(\frac{c_{2N}}{\lambda_2} - \frac{c_{1N}}{\lambda_1}\right) \\ \left(\frac{c_{32}}{\lambda_3} - \frac{c_{12}}{\lambda_1}\right) & \left(\frac{c_{33}}{\lambda_3} - \frac{c_{13}}{\lambda_1}\right) - 1 & \dots & \left(\frac{c_{3N}}{\lambda_3} - \frac{c_{1N}}{\lambda_1}\right) \\ \vdots & \vdots & \ddots & \vdots \\ \left(\frac{c_{N2}}{\lambda_N} - \frac{c_{12}}{\lambda_1}\right) & \left(\frac{c_{N3}}{\lambda_N} - \frac{c_{13}}{\lambda_1}\right) & \dots & \left(\frac{c_{NN}}{\lambda_N} - \frac{c_{1N}}{\lambda_1}\right) - 1 \end{bmatrix} \hat{y}_{i=1} \quad (26)$$

Once we train the system with Hebbian rule, we obtain the synapse matrix and we can compute \mathbf{A} . For the example of patterns “5” and “7” in Fig. 2, numerical analysis shows that the real part of each eigenvalue of \mathbf{A} is negative. Based on stability theory [12], patterns “5” and “7” are therefore both stable equilibria of the proposed ONN system.

C. Robustness against Uniform Transmission Delays

When taking uniform transmission delay δ into account, the input signal from the view of neuron i is $\sum_{j=1}^N s_{ij} e^{i(\theta_j + \delta - \theta_i)}$. The dynamics near the memorized pattern is

$$\begin{aligned} \dot{\theta}_i &= k\theta_{cross}(\hat{s}_i, (\hat{\theta} + \delta\vec{1}) - \theta_i\vec{1}) \\ &= k \cdot \text{atan2}\left(\sum_{j=1}^N s_{ij} \sin(\theta_{ji} + \delta), \sum_{j=1}^N s_{ij} \cos(\theta_{ji} + \delta)\right) \end{aligned} . \quad (27)$$

Near the memorized pattern, $\forall i, \sum_{j=1}^N s_{ij} \cos(\theta_{ji}^* + \delta) > 0$ still holds. We add a small perturbation $\hat{\theta}$ to $\hat{\theta}^*$, and we have

$$\dot{\theta}_i = k \left[\arctan \frac{\sum_{j=1}^N s_{ij} \sin(\theta_{ji}^* + \theta_{ji} + \delta)}{\sum_{j=1}^N s_{ij} \cos(\theta_{ji}^* + \theta_{ji} + \delta)} \right]. \quad (28)$$

It is straightforward to check that $\frac{d}{d\delta} \theta_{cross} = 1$, meaning that near the memorized pattern, θ_{cross} has a linear relationship to δ . Now, (28) becomes

$$\dot{\theta}_i = k \left[\arctan \frac{\sum_{j=1}^N s_{ij} \sin(\theta_{ji}^* + \theta_{ji})}{\sum_{j=1}^N s_{ij} \cos(\theta_{ji}^* + \theta_{ji})} \right] + k\delta. \quad (29)$$

The above equation indicates that at the memorized pattern point, all the neurons have the same frequency offset $k\delta$, the system synchronizes at the frequency of $\Omega + k\delta$. Now, let's consider the dynamics w.r.t. \hat{y} :

$$\begin{aligned} \dot{y}_i &= \dot{\theta}_i - \dot{\hat{\theta}}_i \\ &= k \left[\arctan \frac{\sum_{j=1}^N s_{ij} \sin(\theta_{ji}^* + \theta_{ji})}{\sum_{j=1}^N s_{ij} \cos(\theta_{ji}^* + \theta_{ji})} \right] + k\delta - k \left[\arctan \frac{\sum_{j=1}^N s_{1j} \sin(\theta_{j1}^* + \theta_{j1})}{\sum_{j=1}^N s_{1j} \cos(\theta_{j1}^* + \theta_{j1})} \right] - k\delta \\ &= k \left[\left(\sum_{j=2}^N \left(\frac{c_{ij}}{\lambda_i} - \frac{c_{1j}}{\lambda_1} \right) y_j \right) - y_i \right] \end{aligned}$$

The frequency offset $k\delta$ effectively gets cancelled out and the dynamics is not affected by the uniform transmission delays. The dynamics w.r.t. \hat{y} remains unchanged

$$\dot{\hat{y}}_{i=1} = k\mathbf{A}\hat{y}_{i=1}.$$

Therefore, the memorized patterns are also stable equilibria of the system. The proposed ONN is thus robust against uniform transmission delays.

IV. HARDWARE IMPLEMENTATION FOR UNIFORM TRANSMISSION DELAYS

A. Type-II PLL ONN Architecture

The zero-crossing phase detection ONN model can be achieved in hardware through the Type-II PLL ONN architecture. In this architecture, the multiplier in the original system is replaced by D-flip-flop based phase frequency detector (PFD). The output of PFD only contains the phase difference information between the rising zero-crossing points of input signal and feedback signal. Thus, the Type-II PLL ONN is a practical implementation of the proposed model (15).

This architecture is centered around a Type-II PLL, where the phase difference is measured using a digital phase-frequency detector (PFD) based on D-flip-flops. The standard digital circuit of PFD can be built by using two D-flip-flops and an “AND” gate, as shown in Fig. 8. We refer to [13] for detailed design information. The input-output characteristics of the PFD and the integrator following it provide the Type-II PLL with excellent acquisition range and nearly zero phase error when locked.

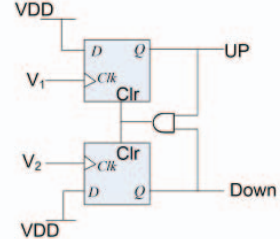


Fig. 8 Conceptual structure of the phase-frequency detector (PFD). The output of the PFD feeds into a charge pump which provides control voltage for VCO.

Other parts of the Type-II PLL include the charge pump combined with a RC loop filter and VCO as detailed in [13]. The simplified structure of the Type-II PLL ONN is shown in Fig. 9.

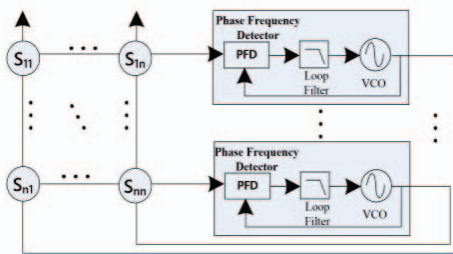


Fig. 9 Simplified Type-II PLL ONN using PFD as the phase detector. For simplification, the charge pump and RC filter are included in the “Loop Filter” block.

B. Robustness against Uniform Transmission Delays

We provide the simulation outcomes to compare the

proposed Type-II PLL ONN with the original ONN under uniform delay conditions. A Type-II PLL ONN behavioral model with 20 neurons was built with the training patterns in Fig. 2. In the uniform transmission delay testing, Type-II PLL ONN synchronizes whereas the original ONN remains in clustered states. The uniform transmission delays are set to be $\delta = 7.2$ degree in this example.

In the experiment, the delay values are uniformly set and the objective pattern is “5”. The objective pattern along with the synapse matrix determines **C** which suggests how many clusters are formed and which neuron belongs to which cluster. Fig. 10 shows the frequency evolution for experiment. The natural frequency decides the initial frequency. We compensate this common frequency mode and only consider the frequency deviation. So when entering evolution stage, all curves start from zero. The initial condition is pattern “5”.

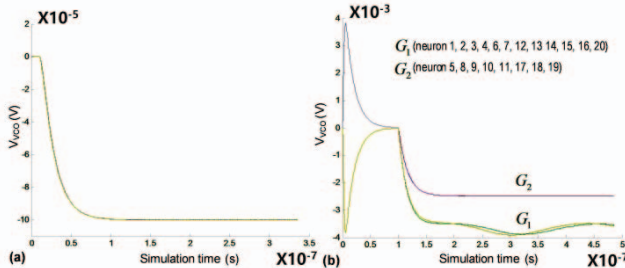


Fig. 10 Simulation of VCO control voltage over time for experiment with “5” as the objective pattern. (a) Behavior of Type-II PLL ONN architecture. (b) Behavior of original ONN architecture.

In Fig. 10 (a), the normalization feature in the Type-II PLL removes the frequency difference at the pattern point and the macro effect is the global synchronization. In Fig. 10 (b), the original ONN evolves into clustered state. The cluster distribution precisely matches the property of matrix **C**. Due to the influence of input amplitude, there is no stable equilibrium near the memorized pattern point.

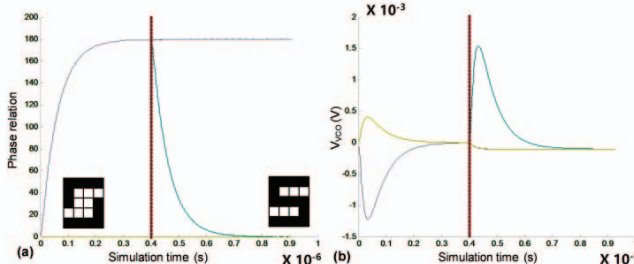


Fig. 11 The retrieval of pattern in Type-II PLL ONN with uniform transmission delays. For a VCO natural frequency of 1 GHz the system retrieves the memorized pattern in about 400 ns. (a) Phase relation vs. time. (b) VCO control voltage (V_{VCO}) vs. time.

With uniform transmission delays, the memorized pattern maintains its stability in Type-II PLL ONN as is proven in Section III. (C). In Fig. 11, the Type-II PLL ONN system initializes at a distorted pattern and the correct pattern is retrieved in the simulation. Due to the delay, there is a constant frequency offset for all neurons at the end of the evolution.

V. HARDWARE IMPLEMENTATION FOR RANDOM TRANSMISSION DELAYS

In an actual hardware system, the transmission delays will be non-uniform. Unfortunately, simulations show that under random delays, both proposed and original systems fail to synchronize and instead evolve into clusters. What's worse, the clustering can be affected by different transmission delays, and therefore changes for different weight patterns and hardware variations. Thus, the unknown and complex phase noise environment in real hardware system makes the ONN performance hard to predict.

To tackle this problem, we develop a technique to ensure uniform transmission delays and make the system much more robust against random transmission delays in real system.

A. Phase Correction Technique

The idea of the phase correction technique is to “snap” the phase shift in the summed signal to a quantized value, such that the transmission delays viewed by each neuron are uniform.

This idea can be implemented using a synchronous comparator clocked at a higher frequency than the neuron output. The D-flip-flop is a typical circuit for such function. The D-flip-flop captures the value of the D-input at a defined portion of the clock cycle (here we choose the rising edge of the clock). The captured value becomes the Q output. At other times, the output Q does not change.

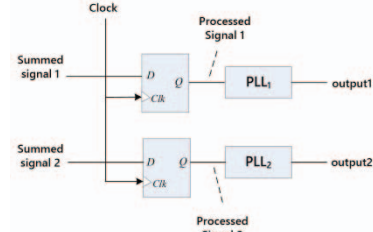


Fig. 12 Conceptual structure of the phase correction technique with D-flip-flops.

The conceptual design of the phase correction technique is shown in Fig. 12. The summed signals are processed by the D-flip-flop before received by neurons. The clock port (*Clk*) is hooked up to a high frequency clock. D-flip-flop samples and compares the summed signal at every rising edge of the clock.

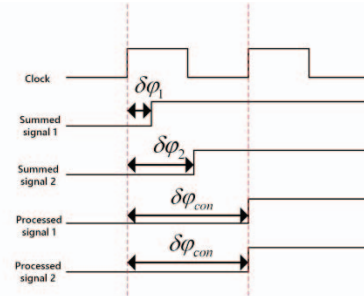


Fig. 13 Timing diagram showing the mechanism of the phase correction technique.

The timing diagram in Fig. 13 illustrates the mechanism of the phase correction technique. Neuron 1 and neuron 2

should be in-phase under ideal condition, but different transmission delays ($\delta\varphi_1$ and $\delta\varphi_2$) distort the phase information in the summed signals. The D-flip-flop samples the summed signal at the second rising edge of the clock and delivers this signal to the neuron. The equivalent effect is that each neuron receives the summed signal with uniform transmission delay $\delta\varphi_{con}$. With uniform transmission delays, synchronization will occur as long as $\delta\varphi_i$ are smaller than the sampling clock period. This allows a system to be designed with clear metrics for guaranteeing synchronization that is not dependent on the synaptic pattern.

B. Proposed Phase Correction Architecture

Here we design an architecture applying the snapping technique to the Type-II PLL ONN.

From the practical view point, we want to simplify the circuit design and minimize the cost of power and the number of components. One request is to avoid the use of on-chip global clock source. In Fig. 14, the local clock phase correction architecture is presented.

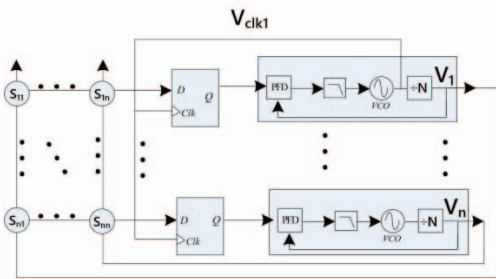


Fig. 14 Local clock phase correction architecture using the local high speed signal of neuron 1 as the global reference clock.

This architecture replaces the global clock source with the local clock of one of the neurons (we choose neuron 1 as an example). Neuron 1 serves as the sampling and quantization reference of the whole network. Different from the previous structure, the PLL here must be equipped with a divider to divide the VCO output by N . Thus, the VCO will operate at high frequency which can be used as the local clock source. V_{clk1} is the high speed local signal while $V_{1\dots n}$ are lower-speed signals that contain the phase information in the ONN. V_{clk1} serves as the global reference clock, and $f_{V_{clk1}} = N f_{V_{1\dots n}}$.

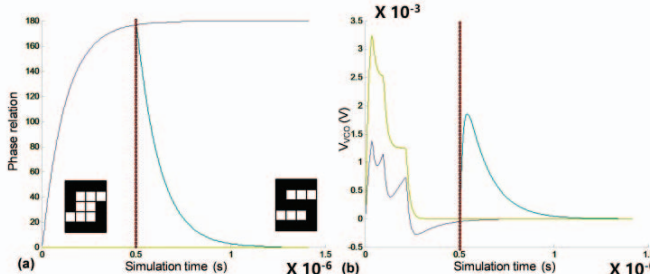


Fig. 15 Performance of proposed ONN with local clock phase correction structure.

In the simulation experiments, the transmission delays are randomly set (each delay is smaller than 30 degrees in the experiments). The performance of this architecture in one experiment is shown in Fig. 15. We can see that the ONN

successfully converges to correct pattern.

VI. CONCLUSION

The major contributions of this paper consist of four aspects. First, the frequency clustering phenomenon in ONNs with transmission delays has been described and explained. Second, a novel ONN architecture has been proposed and studied for mitigation of this phenomenon. The architecture has been shown to be robust against uniform transmission delays. Third, a practical implementation of the proposed ONN model in hardware has been designed and simulated. Finally, a phase correction technique to ensure frequency synchronization as well as the correct phase relation convergence in the presence of random delays has been proposed and demonstrated that will make actual hardware implementation feasible. Our work provides theoretical understanding and practical implementation methods to enable design of ONNs on ICs for statistical information processing.

REFERENCES

- [1] H. Li, X Liao, C Li, H Huang, and C Li, "Edge detection of noisy images based on cellular neural networks," *Commun. Nonlinear Sci. Numer. Simul.*, vol. 16, no. 9, pp. 3746-3759, Sept. 2011.
- [2] T-J Su, J-C Cheng, M-Y Huang, T-H Lin, and C-W Chen, "Applications of cellular neural networks to noise cancellation in gray images based on adaptive particle-swarm optimization," *Circuits Syst. Signal Process.*, vol. 30, no. 6, pp 1131-1148, Dec. 2011.
- [3] K. Andrej, T. George, S. Sanketh, L. Thomas, S. Rahul, and F. F. Li, "Large-scale Video Classification with Convolutional Neural Networks," in *Proc. IEEE Conf. Comput. Vis. Pattern Recog.*, pp. 1725-1732, Jun. 2014.
- [4] P. Kinget and M. S. J. Steyaert, "A programmable analog cellular neural network CMOS chip for high speed image processing," *IEEE J. Solid-State Circuits*, vol. 30, no. 3, pp. 235-243, March 1995.
- [5] J. M. Cruz and L. O. Chua, "A 16x16 cellular neural network universal chip: the first complete single-chip dynamic computer array with distributed memory and with gray-scale input-output," *Analog Integrated Circuits and Signal Process.*, vol. 15, no. 3, pp. 227-237, March 1998.
- [6] F. C. Hoppensteadt and E. M. Izhikevich, "Pattern recognition via synchronization in phase-locked loop neural networks," *IEEE Trans. Neural Netw.*, vol. 11, no. 3, pp. 734-738, May 2000.
- [7] T. Jackson, A. Sharma, J. Bain, J. Weldon, and L. Pileggi, "Oscillatory Neural Networks Based on TMO Nano-Oscillators and Multi-Level RRAM Cells," *IEEE J. Emerg. Sel. Topics Circuits Syst.*, vol. 5, no. 2, pp. 230-241, June 2015.
- [8] V. Calayir and L. Pileggi, "Device Requirements and Technology-Driven Architecture Optimization for Analog Neurocomputing," *IEEE J. Emerg. Sel. Topics Circuits Syst.*, vol. 5, no. 2, pp. 162-172, June 2015.
- [9] T. Nishikawa, Y.-C. Lai, and F.C. Hoppensteadt, "Capacity of oscillatory associative-memory networks with error-free retrieval," *Phys. Rev. Lett.*, 92, pp. 108101, March 2004.
- [10] M. K. S. Kunyosi and L. H. A. Monteiro, "Recognition of noisy images by PLL networks," *Signal Process.*, vol. 89, no. 7, pp. 1311-1319, July 2009.
- [11] F. G. Kazanci and B. Ermentrout, "Wave Formation through the Interactions between Clustered States and Local Coupling in Arrays of Neural Oscillators," *SIAM J. Appl. Dyn. Syst.*, vol. 7, no. 2, pp. 491-509, May 2008.
- [12] H. K. Khalil, *Nonlinear Systems*, 3rd ed., New Jersey: Prentice hall, 2002.
- [13] B. Razavi, *Design of Analog CMOS Integrated Circuits*, Singapore: McGraw-Hill, 2001.